Chapter II

Theoretical Part

2.1 Chemical Durability of Glass

The term 'chemical durability' has been used conventionally to express the resistance offered by a glass towards attack by aqueous solutions and atmospheric agents. There is no absolute or explicit measure of chemical durability. However, the chemical durability of a formed glass article can be improved by lowering the alkali content of the surface of the article before use.

2.1.1 Reactions Mechanism of Glasses with Aqueous Solution

When a piece of ordinary glass is brought into contact with an aqueous solution, 3 types of process will occured. These are leaching, network dissolution and compound formation of reaction product.

1. Leaching Mechanism

In this process, an alkali or alkali earth were replaced by ion exchange between hydrogen (or hydronium) ions from the water. This can result in the formation of a hydrated silica rich layer on the surface of the glass.

$$\equiv Si\text{-}O\text{-}Na^{+}(glass) + H^{+}(aq) \longrightarrow \equiv Si\text{-}OH(glass) + Na^{+}(aq) \quad (2.1)$$

Within the glass, two hydroxyl groups recombine to form a ≡Si-O-Si≡ bridge and an intersticial water molecule. The former one leads to

an improved resistance of the leached layer towards dissolution, the latter one to an enhanced mobility within the ion exchange layer. Usually, the total release of leached matter is presented in terms of q in mg/cm^2 and this value is proportional to $\sqrt{t}$. An overall diffusion coefficient D can be attributed to the leaching process.

2. Network Dissolution

The dissolution of alkali-silicate and alkali-lime-silicate glasses by aqueous solutions can be described in terms of three chemical reactions:

(a) In the alkali range, the hydroxyl ion in solution disrupts siloxane bonds in the glass:

$$\equiv Si\text{-}O\text{-}Si + OH^- \longrightarrow \equiv Si\text{-}OH + \equiv Si\text{-}O^- \quad \text{----------(2.2)}$$

and the non-bridging oxygen radical formed in reaction (2.2) interacts with a further molecule of water producing a hydroxyl ion, which is free to repeat the reaction (2.2) again (OH^- catalyzed reaction) :

$$\equiv Si\text{-}O^- + H_2O \longrightarrow \equiv Si\text{-}OH + OH^- \quad \text{----------(2.3)}$$

(b) In the acid range, the proton disrupts the siloxane bonds,

$$\equiv Si\text{-}O\text{-}Si\equiv \text{ (glass)} + H^+(aq) \longrightarrow \equiv Si^+ + HO\text{-}Si\equiv \quad \text{--(2.4)}$$

$$\equiv Si^+ + H_2O \longrightarrow \equiv SiOH + H^+ \quad \text{----(2.5)}$$

As the H^+ appears at the end again, this reaction is H^+ catalyzed. The pH value of the reaction divides which process predominates. Both the OH^- and H^+ catalyzed reactions have to pass through a state of activation, i.e., an activated complex. This may be illustrated as

$$\equiv Si\text{-}O\text{-}Si\equiv \xrightarrow{OH^-} \quad \text{or} \quad \equiv Si\text{-}O\text{-}Si\equiv \xrightarrow{H^+}$$

respectively. In either case, the mobility of the proton is rate determining. The activation energy remains within a narrow range from 70 to 80 kJ/mol. The weight loss per surface area q due to the above mechanisms is a linear function of time. So we can formulate a constant dissolution velocity

$$v = (1/\rho)(q/t) \sim q/(\rho.t) \qquad \text{----------(2.6)}$$

(c) Ions in solution are able to interfere with the mechanisms described in (a) and (b). Even traces of Al^{3+} or Zn^{2+} considerably reduce q. By contrast, high concentrations of neutral alkali salts enhance q.

(d) The reaction in hydrofluoric acid is only apparently similar to the OH^- catalyzed reaction.

$$\equiv Si\text{-}O\text{-}Si\equiv \xrightarrow{H\text{-}F} \equiv Si\text{-}F + HO\text{-}Si\equiv \qquad \text{----------(2.7)}$$

$$SiO_2 + 6HF \longrightarrow H_2SiF_6 + 2H_2O$$

low conc. $\rightleftharpoons$ high conc.

$$SiF_4 + 2HF + 2H_2O \qquad \text{----------(2.8)}$$

(e) Simultaneous action of network dissolution and leaching makes the leached layer (ion exchange zone) assume a steady state depth d, $d = D/v$.

(f) The leached or dissolved matter from the glass eventually accumulates in the solution and changes its activities. If a solubility limit is reached, then compound formation

and precipitation will occur, preferentically in the vicinity of the glass surface. That is why the amount of solution available per 1 cm^2 of glass surface is an important parameter for the reaction between glass and aqueous solutions.

The mechanisms of leaching and network dissolution are show in the figure below.

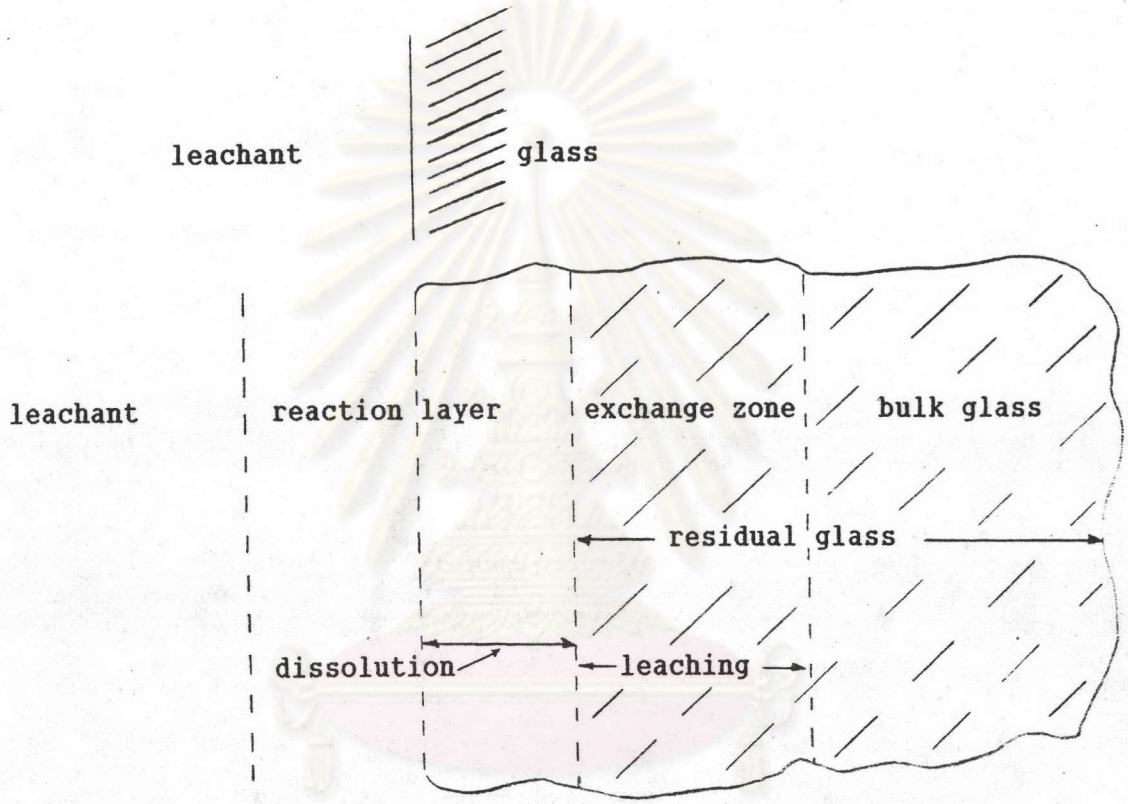

Fig 2.1 Reaction mechanisms; leaching and network dissolution of glass in aqueous solution.

3. Weathering

A dirty window from raining was an example. This occurs by a reaction of water and window as discribed in the following figure.

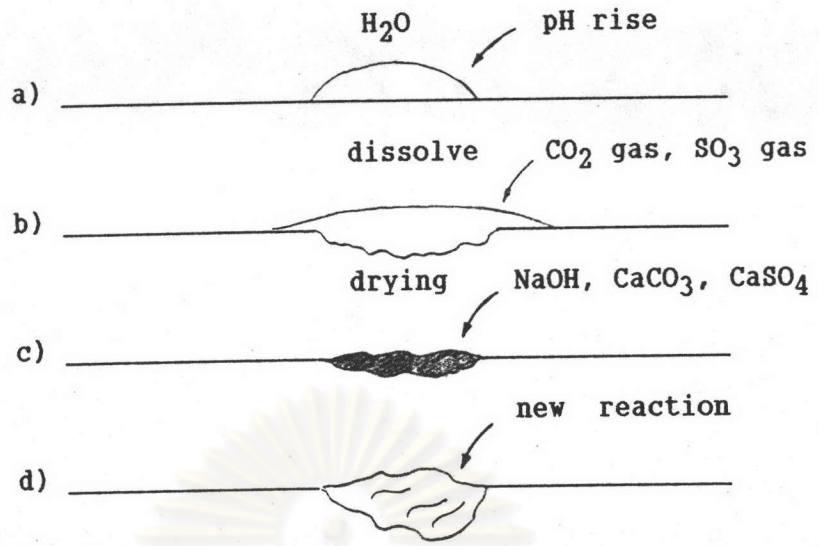

Fig 2.2 Wheathering process on glass surface.

Weathering is a case of extreamly low amounts of water per glass surface area.

2.1.2 Factors Influencing the Chemical Durability

2.1.2.1 The s Factor

As mentioned above, the s factor is the ratio of the surface area of the glass to volume of the leaching solution in the unit of cm^{-1}. When a large excess of solution is used, the s factor will go to zero. Dimbleby and Turner (see Paul, 1982) studied about the quantity of material extracted from a silicate glass varying with the ratio of surface area of glass to the volume of the leaching solution. The results show that the pH of the solution increases when the ratio of the surface area of the glass to the volume of the solution is increased. The increase in the pH enhances the network dissolution velocity. By contrast, accumulated reaction products can slow down the dissolution velocity in a closed system to almost zero.

2.1.2.2 The Frequency of Replenishing Solution

An experiment was carried out by Shamy,1966 to study the effect of frequency of replenishing the leaching solution on the alkali and silica extracted from a glass under certain conditions. The results show a marked increase in the amount of silica extracted as the number of replenishing times is decreased. Later studies showed that this is due to the pH increase. For really long exposure times, the amount of dissolved silica decrease the dissolution velocity approximately proportional to (1-C/Cs), where C and Cs is the actual and saturation concentration of silica. Upon frequent replenishment, or in a flow experiment, or for s-->o, the so-called initial dissolution velocity v_o is measured.

2.1.2.3 Temperature

Both the quantity of dissolved glass matter and alkali extracted from a glass increase with increasing temperature. Some workers have attempted to express the temperature-dependence of alkali extraction in terms of the Arrhenius equation:

$$A = Be^{-E/RT} \qquad \text{----------(2.9)}$$

Where A is the specific reaction rate changing with temperature, B is a constant, R the gas constant, T the absolute temperature, and E the activation energy; E is due to proton transfer. (see 2.1.1)

2.1.2.4 The pH of the Solution

The chemical durability of silicate glass critically depends on the pH and the nature of the attacking solution. When an alkali-silicate glass is placed in pure water, the water

instantaneously becomes a solution of alkali oxide and silica. The pH of solution depends on the concentration of alkali or the ratio of alkali oxide to silica in the glass.

The effect of the different pH values of the solution on the decomposition of simple glasses, and the rate at which the constituents of the glass go into solution, has been studied by Lewins(1965). These results showed that all silicate glasses usually decompose above pH ~ 9-10. Figure 2.3 show the rate of extraction of Mclnnes-Dole glass samples as a function of the pH. (Boksay and Bouquet, 1980)

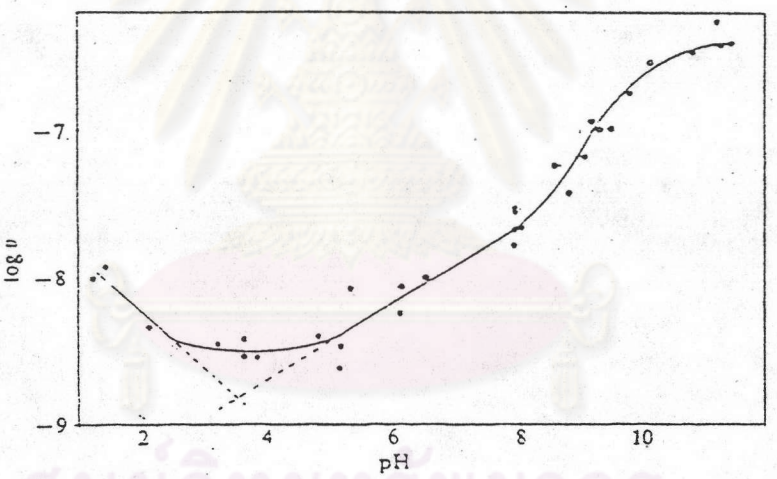

Fig 2.3 Dissolution rate of Mclnnes-Dole samples as a function of the pH.

2.1.2.5 Geometry of Glass Sample

The difference in geometry of the same glass composition will yield a different shape factor. This can influence the dissolution of glass such as fibre and chip glass sample. Let the reaction proceed at the constant velocity v. For fibres which have

cylindrical shape;

$$\alpha = 1 - m_{rest}/m_o \qquad \text{----------(2.10)}$$

when α = reaction progress

m_o = initial mass = $\pi\rho Lr^2$

m_{rest} = mass still unreacted = $\pi\rho L(r_o-vt)^2$

so; $$\alpha = 1-(r_o-vt)^2/r_o^2$$

$$= 1-(1-vt/r_o)^2$$

$$vt/r_o = 1-(1-\alpha)^{1/2} = t/t_* \qquad \text{----------(2.11)}$$

or; $$1-(1-\alpha)^{1/2} = 0.2929\ t/t_{0.5} \qquad \text{----------(2.12)}$$

$$\alpha = 0.084...t^2/t_{0.5}^2$$

When t_* = time for complete reaction

$t_{0.5}$ = haft time; time where α = 0.5

An example of a fibre dissolving and forming a reaction layer is shown in the following figure.

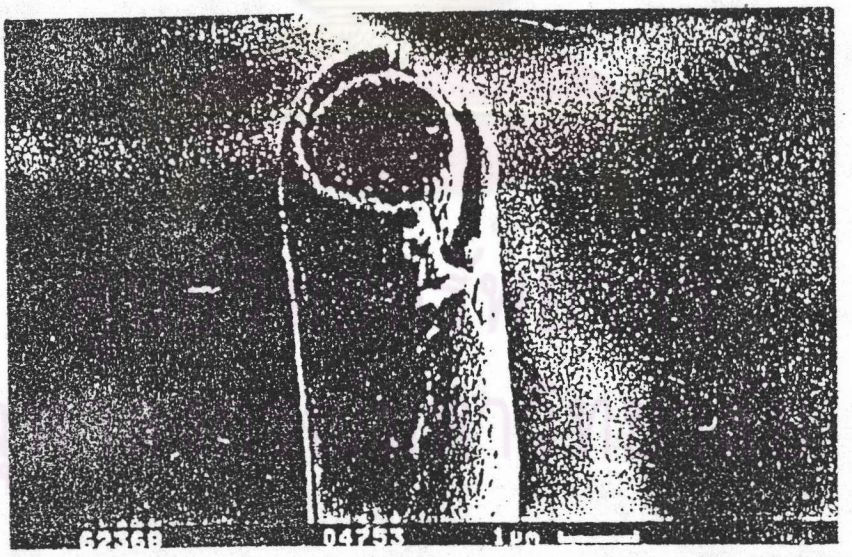

Fig 2.4 Dissolution of fibre (cylendrical shape)

The same approach for chip or plane sheet sample leads to

$$\alpha = t/t_* = 0.5\ t/t_{0.5} \qquad \text{----------(2.13)}$$

2.1.2.6 Surface Condition

A different surface condition such as binder coating will also effect the dissolution of glass. The reaction of binder and glass surface is shown in the following figure. The effect reported is often contradictory, i.e., sometimes an enhanced corrosion rate is found, sometimes a retarded one.

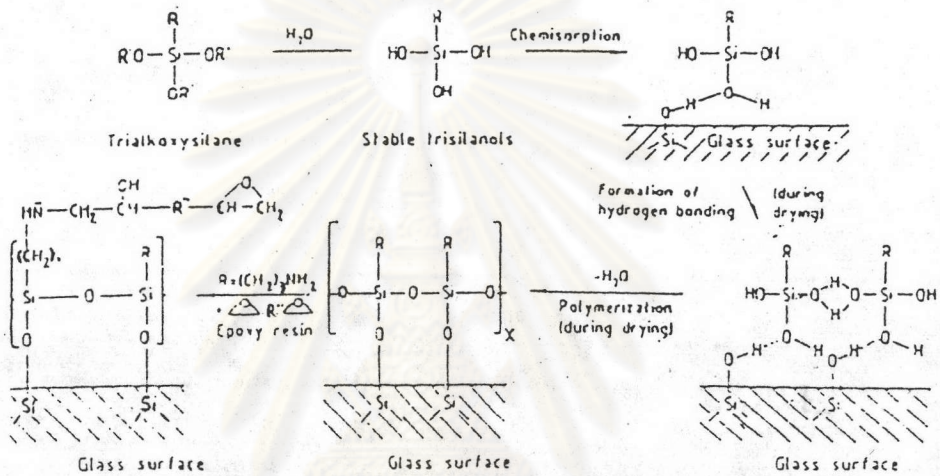

Fig. 2.5 Effect of binder on glass surface.

2.1.3 The Thermodynamics of Multicomponent Glasses

There are two types of stability to be distinguisted.

(a) Thermodynamic stability: The system is in equilibrium corresponding to minimum possible free energy, the system is stable in the strict sense, that is none of the conceivable changes in the system can occur spontaneously. Time is not a parameter for this type of stability.

(b) Kinetic stability: The system is not in a state of equilibrium, some changes can occur spontaneously but at an slow rate. So, the time demand for the respective change becomes the key issue. Such systems are considered as stable if no changes occur

within historical times. The best possible example of kinetic stability is the existence of glass itself.

For the chemical durability of glass, there may be some arguments that it should be a matter of thermodynamic equilibrium as well as kinetic stability. So, in reality the durability of glass may be expressed as a function of both thermodynamic and kinetic stability:

Durability = f(kinetic stability) x f(thermodynamic stability)

The relative influence of either of these two factors on durability will depend on the nature of the test. In a general form, the dissolution velocity v(t) takes the form

$$v(t) \sim X_o.\exp(-Ea/RT).\exp(-G_{hyd}/RT).(1-C/Cs) \quad \text{----------(2.14)}$$

kinetic term thermodynamic term.

C = actual concentration of silica

Cs = saturation concentration of silica in the closed system

X_o = kinetic function

G_{hyd} = Gibbs free energy of hydration

In closed systems, or with large s.t values, G_{hyd}, C, and Cs are function of v.t. In flow experiments, or with small s.t values, G_{hyd}, and Cs are constant, and C<<Cs. Ea~70-80 kJ/mol for most glasses. Grambow (1985) has shown that the kinetic term is approximately the same function for very different glasses : $X_o \sim 8.2$ cm/s. So the difference of stability in open systems mainly depends on G_{hyd}.

From the above discussion it is clear that a large

increase of either thermodynamic or kinetic stability will make the glass more durable. In the limiting case, it could be argued that in the case of thermodynamic stability or equilibrium, the chemical potentials of the species on the glass surface and those in solution are equal and thus no net mass transfer would take place. However, it has been shown that due to the Gibbs free energy difference between glass and crystal, such a state is never reached until all glasses have reacted.

The glass dissolving process can be approached by the reaction

$$\text{glass + water} \xrightarrow{\Delta G_{hyd}} \text{aqueous reaction products} \quad \text{-----(2.15)}$$

The Gibbs free energy of formation of this reaction can predict a dissolution rate when compaired with another glass. In order to calculate ΔG_{hyd} from thermodynamic data, a simplified thermodynamic cycle was created as show in the following figure (see next page)

According to the figure, the following balance holds:

$$\Delta G_{hyd}(glass) = G^f(products) - G^f(glass)$$
$$= \Sigma G^f(product) - \Sigma G^f(compound) - \Delta G^{mix} \quad \text{---(2.16)}$$

$$\Delta G^{mix} = G^{mix,id} + G^E \quad \text{---------(2.17)}$$

Where ΔG^{mix} is the Gibbs free energy of mixing the compounds to a homogeneous glass. $G^{mix,id}$ is the mere statistical part (configurational part).

$$G^{mix,id} = RT \Sigma xj \ lnxj. \quad \text{---------(2.18)}$$

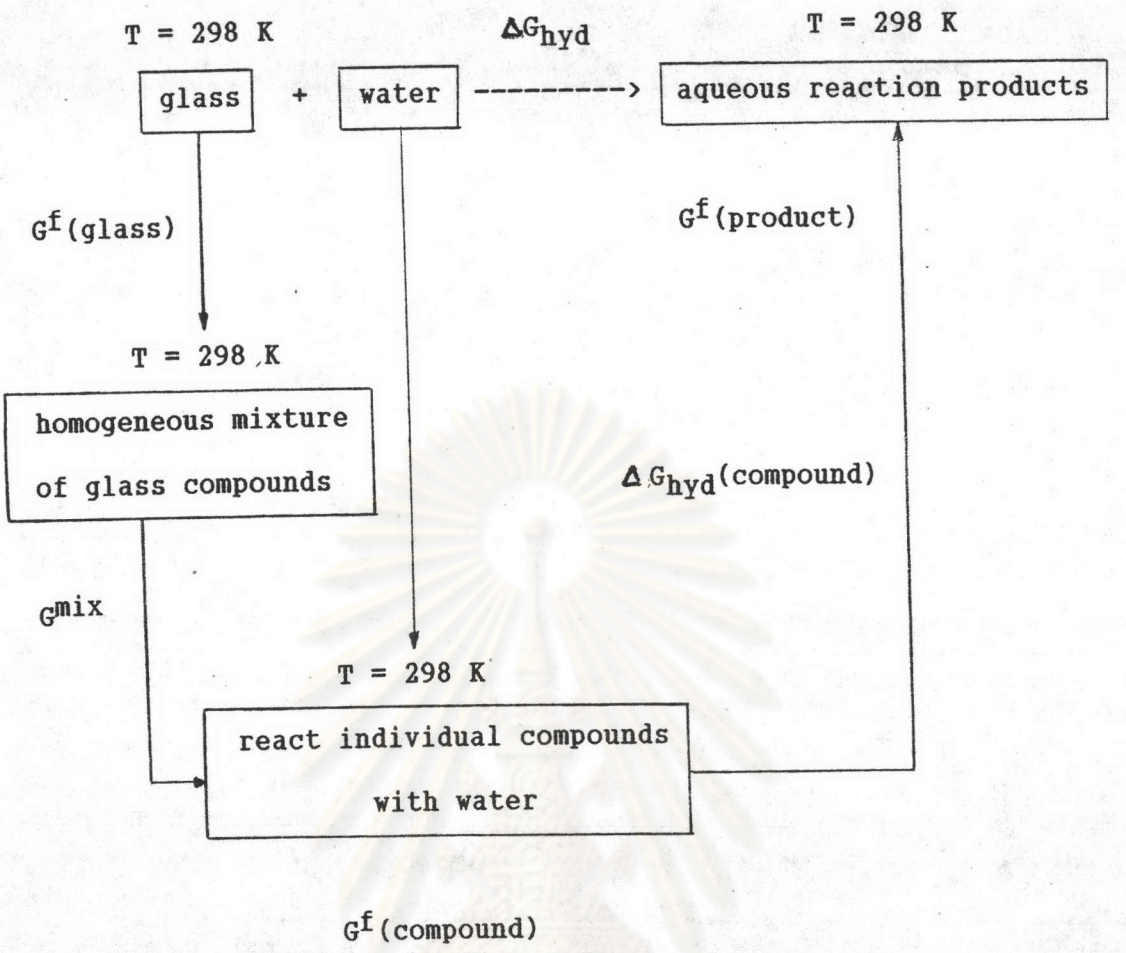

Fig. 2.6 Thermodynamic cycle of glass dissolving process.

It only depends on the molar fractions xj of the components j, not on their nature. The term G^E allows for reactive mixing. Now it is true that j must not be chosen as the oxides in the glass since these react heavily and make a large G^E. However, G^E can be minimized and neglected if we choose the set of compounds j in such a way that they do not react chemically among each other. Such a distinguisted set of compounds is seen in the coexisting compounds given by the phase diagrams of the respective oxide systems of the glass.

ΔG_{hyd}(compound) = Gibbs free energy of hydration of compound (kJ/mol)

ΔG_{hyd}(glass) = Gibbs free energy of hydration of glass (kJ/100g)

G^{mix} = Gibbs free energy of mixing

$G^{mix,id}$ = Gibbs free energy of ideal mixing

G^{E} = excess Gibbs free energy

2.2 Speciation of Aqueous Phase

The occurrence of certain species in an aqueous medium depends on the pH value as well as on the presence of ions . All species are present in infinite dilution and no interaction among different species are taken into account. No reaction partners other than H^+, OH^- and H_2O, dissolved CO_2 are presented (see 2.2.2). More details are elaborated in the following section.

2.2.1 Thermodynamic Concept

Consider a chemical reaction

$$aA + bB \longrightarrow cC + dD \qquad \text{----------(2.19)}$$

The relationship between the equilibrium constant K and the free energy change of the relation is

$$\Delta G = \Delta G^{o} + RT \ln K$$

In equilibrium, ΔG assumes the value zero, $\Delta G = 0$ and therefore

$$\Delta G^{o} = -RT \ln K \qquad \text{----------(2.20)}$$

In (2.20) R is the gas constant, T the absolute temperature; at T = 298 K therefore, G given in units of cal:

$$\Delta G^{o} = -1.987 \text{ cal.K}^{-1} \times 298.15 \text{ K} \times 2.303 \log Kp$$

$$= 1364.35 \log Kp$$

or $$\log K_p = -\Delta G^{o} / 1364.35 \qquad \text{----------(2.21)}$$

2.2.2 Stability Diagrams

It is well known that pH can effect the corrosion of glasses (see 2.1.2.4) and also the reaction of oxides and standard Gibbs free energy (ΔG^{o}) can be found when G^{o} of each species were known. This leads to a plot between log activity and pH from 0 to 14 which is called 'stability diagram'. From this diagram, it can be predicted which species will occur in the selected pH range. The stability diagram of silica is selected as an example.

2.2.2.1 Stability Diagram of Silica

The relative solubility of silica in water is one of the main factors in the corrosion of glass. When silica (quartz) is brought into contact with water at ordinary temperatures, the value of the equilibrium solubility is very low (~6 ppm for quartz). In principle the thermodynamic stability of a glass may be considered to be the stability of its coexisting compound j and the equilibrium constants of hydration, ionization and complexation.

With the available thermodynamic data (see table 2.1) it is possible to calculate the various energy changes being associated with these processes, and therefore the stability of the glass under various conditions can be found from the equilibrium constant K in terms of the activities of the reaction products stemming from the divese oxides.

Table 2.1a Gibbs free energies G of aqueous species of selected oxides at T=298 K.

oxides	species	-G in Kcal/mol	oxide	species	-G in Kcal/mol
Al_2O_3	Al_2O_3	376.77	CdO	CdO	53.79
	Al^{3+}	117.59		Cd^{2+}	18.58
	$Al(OH)^{2+}$	167.46		$HCdO_2^-$	86.50
	$Al(OH)_2^+$	216.87		$Cd(OH)^+$	64.90
	$Al(OH)_3$	265.55		$Cd(OH)_2$	122.46
	$Al(OH)_4^-$	312.00		$Cd(OH)_3^-$	144.60
	AlO_2^-	200.70		$Cd(OH)_4^{2-}$	181.60
	$Al(SO_4)^+$	299.48		$CdCl_2$	85.00
	$Al(SO_4)^-$	479.84		$CdSO_4$	199.50
	$Al_2(SO_4)_3$	735.31		$CdCO_3$	160.00
B_2O_3	B_2O_3	280.40(g)	CO_2	CO_2	92.26
	H_3BO_3	230.16		H_2CO_3	148.94
	$H_2BO_3^-$	217.63		HCO_3^-	140.26
	HBO_3^{2-}	200.29		CO_3^{2-}	126.71
	BO_3^{2-}	181.48	CaO	CaO	144.40
BaO	BaO	126.30		Ca^{2+}	132.18
	Ba^{2+}	130.86		$Ca(OH)^+$	171.55
	$Ba(OH)^+$	171.48		$Ca(OH)_2$	207.49
	$Ba(OH)_2$	209.20		$CaSO_4$	313.20
	$BaSO_4$	311.86		$CaCO_3$	262.64
	$BaCl_2$	196.70		$CaCl_2$	195.04
	$BaCO_3$	272.20		$CaHCO_3^+$	273.67

Table 2.1b Gibbs free energies G of aqueous species of selected oxides at T=298 K.

oxides	species	-G in Kcal/mol	oxide	species	-G in Kcal/mol
Cr_2O_3	Cr_2O_3	253.30	Li_2O	Li_2O	133.90
	Cr^{3+}	53.35		Li^+	69.94
Fe_2O_3	Fe_2O_3	176.77		$Li(OH)$	107.82
	Fe^{3+}	4.27		$LiCl$	101.57
	$Fe(OH)^{2+}$	57.46		Li_2SO_4	317.78
	$Fe(OH)_2^+$	109.28		Li_2CO_3	266.66
	$Fe(OH)_3$	160.30			
	$Fe(OH)_4^-$	201.20	MgO	MgO	136.13
	$FeCl_3$	99.45		Mg^{2+}	108.99
	$FeSO_4^+$	187.71		$Mg(OH)^+$	150.10
	$Fe(HPO_4)^+$	279.59		$Mg(OH)_2$	199.27
	Fe^{2+}	22.05		$MgCO_3$	239.60
	$Fe(OH)^+$	66.91		$MgHCO_3^+$	251.10
	$Fe(OH)_2$	109.20		$MgCl_2$	171.69
	$Fe(OH)_3^-$	148.00		$MgSO_4$	298.63
	$Fe(OH)_4^{2-}$	185.00			
	$FeCl_2$	72.43	MnO	MnO	86.80
	$FeSO_4$	196.10		Mn^{3+}	20.40
	$FeCO_3$	162.40		Mn^{2+}	54.96
				$Mn(OH)^+$	97.20
H_2O	H_2O	56.69		$Mn(OH)_3^-$	178.40
	H^+	0.00		$MnSO_4$	228.48
	OH^-	37.59		$MnCO_3$	195.40

Table 2.1c Gibbs free energies G of aqueous species of selected oxides at T=298 K.

oxides	species	-G in Kcal/mol	oxide	species	-G in Kcal/mol
K_2O	K_2O	76.97	Na_2O	Na_2O	62.59
	K^+	67.47		NaOH	99.23
	KCl	98.82		$NaHCO_3$	202.89
	KSO_4^-	246.36		NaCl	93.94
	KOH	105.06		Na_2SO_4	240.91
P_2O_5	P_2O_5	328.00	SiO_2	SiO_2	192.40
	H_3PO_4	274.20		H_4SiO_4	312.72
	$H_2PO_4^-$	270.17		$H_3SiO_4^-$	299.39
	HPO_4^{2-}	260.34		$H_2SiO_4^{2-}$	283.49
	PO_4^{3-}	243.50		SiO_4^{4-}	250.69
				H_2SiO_3	242.00
PbO	PbO	45.0		$HSiO_3^-$	228.36
	$Pb(OH)^+$	54.10		SiO_3^{2-}	212.00
	$Pb(OH)_2$	95.80			
	$Pb(OH)_3^-$	137.60	SrO	SrO	133.80
	$PbSO_4$	187.20		Sr^{2+}	136.58
	$HPbO_2^-$	81.00		$Sr(OH)^+$	175.30
	$PbCl_2$	75.04		$Sr(OH)_2$	207.80
	$PbCO_3$	149.70		$SrCO_3$	271.90
				$SrSO_4$	318.90
H_2SO_4	H_2SO_4	180.48	TiO_2	TiO_2	212.30
	SO_4^{2-}	177.78		TiO^{2+}	138.00

Table 2.1d Gibbs free energies G of aqueous species of selected oxides at T=298 K.

oxides	species	-G in Kcal/mol	oxide	species	-G in Kcal/mol
	$TiO(OH)_2$	253.00	ZnO	ZnO	76.08
	$HTiO_3^-$	111.70		$Zn(OH)^+$	39.65
				Zn^{2+}	35.18
ZrO_2	ZrO_2	247.70		$Zn(OH)_2$ (cr)	133.31
	Zr^{4+}	142.00		(amorp.)	131.85
	ZrO^{2+}	201.50		$HZnO_2^-$	110.90
	$ZrO(OH)_2$	311.50		$Zn(OH)_3^-$	168.43
	$Zr(OH)_4$	370.00		$Zn(OH)_4^{2-}$	208.24
	$HZrO_3^-$	287.70		$ZnSO_4$	209.00
				$ZnCO_3$	174.85
				$ZnCl_2$	88.30

When silica (quartz) is brought into water the reaction may be represented as

$$SiO_2 \text{ (quartz)} + H_2O = H_2SiO_3 \quad \text{----------(2.22)}$$

$$Kp = [H_2SiO_3] / [SiO_2][H_2O] \quad \text{----------(2.23)}$$

ΔG^o of reaction (2.23) is + 4.69 kcal. Therefore log K_p = -3.44. (see eq 2.21). In this particular case, pure quartz is reacting with pure water, with very little formation of H_2SiO_3, thus

$$[SiO_2] = [H_2O] = 1$$

Therefore

$$[H_2SiO_3] = Kp = 10^{-3.44} \sim [H_2SiO_3]$$

$$\log [H_2SiO_3] = -3.44 \qquad \text{----------(2.24)}$$

From equation (2.24) it will appear that solubility of SiO_2, in terms of H_2SiO_3 in solution, is independent of pH. The dissociation of silicic acid can be written as

$$SiO_2 + H_2O = H_2SiO_3 \quad K1 \quad H^+ + HSiO_3^- \qquad \text{----------(2.25)}$$

$$SiO_2 + H_2O = H_2SiO_3 \quad K2 \quad 2H^+ + SiO_3^{2-} \qquad \text{----------(2.26)}$$

For (2.25), ΔG^o = +18.33 kcal, and log K1 = -13.43

$$K1 = [HSiO_3^-][H^+] \ / \ [SiO_2][H_2O]$$

$$\log K1 = \log [HSiO_3^-] - pH$$

$$\log [HSiO_3^-] = -13.43 + pH \qquad \text{----------(2.27)}$$

This shows that although the solubility of silica near the neutral point (pH~7) is not greatly affected by pH, the solubility increases rapidly with alkalinity at pH > 9. Similarly, for the reaction (2.26), ΔG^o = + 34.69 kcal. and log K2 = -25.43

Thus $\log [SiO_3^{2-}] = -25.43 + 2pH \qquad \text{----------(2.28)}$

With (2.24), (2.27) and (2.28) the equilibrium activity (or, loosely, concentration in mol/l) of different species of silica in aqueous solution has been calulated at various pH values by using computer spread sheet Lotus 123, and these are shown in table 2.2, along with the corresponding solution values for vitrious silica.

SiO2

	SiO2 +H2O =H2SiO3	SiO2 +H2O =HSiO3 - +H+	SiO2 +H2O =SiO3 2- +2H+
f(1)	1.00	1.00	1.00
G(1)	-190.00	-190.00	-190.00
f(H+)		1.00	2.00
f(H2O)	1.00	1.00	1.00
f(2)	1.00	1.00	1.00
G(2)	-242.00	-228.36	-212.00
dG	4.69	18.33	34.69
log Kp	-3.44	-13.43	-25.43

pH	Log a.H2SiO3	Log a.HSiO3	Log -a.SiO3 2-
0.00	-3.44	-13.43	-25.43
0.20	-3.44	-13.23	-25.03
0.40	-3.44	-13.03	-24.63
0.60	-3.44	-12.83	-24.23
0.80	-3.44	-12.63	-23.83
1.00	-3.44	-12.43	-23.43
1.20	-3.44	-12.23	-23.03
1.40	-3.44	-12.03	-22.63

Table 2.2 Different species of silica in aqueous solution at various pH.

The result from table above can be plotted in the following figure.

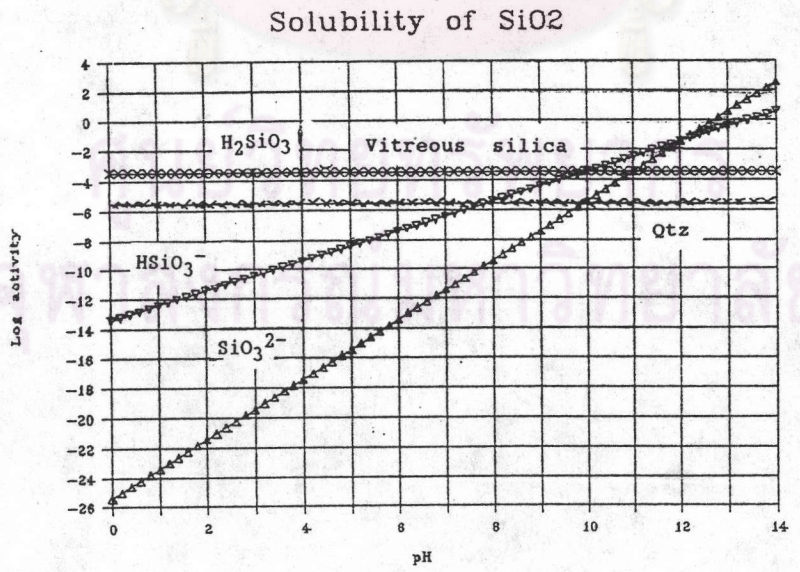

Fig 2.7 Solubility diagram of silica in water.

From the above figure, we can see three distinct pH zones based on the predominance of one particular silicate species. For example, in the first zone (pH<10) the minimum solubility is presented by the undissociated but soluble portion of H_2SiO_3, this species predominates up to pH=10. In the second zone (pH=10 to 12) most of the silica which passes into the solution is due to the formation of $HSiO_3^-$ species. In the third zone (pH>12) SiO_3^{2-} predominates. From the above figure, it is also evident that the quantity of silica extracted from both quartz and vitreous silica follows the same pattern but the solubility of silica from the glassy form is more than that from quartz. This is because the Gibbs free energy of quartz is more negative than that of vitreous silica, or in other words quartz is thermodynamically more stable than vitreous silica.

2.3 Speciation of Glass Phase

Understanding on glass compounds was necessary to calculate the Gibbs free energy of formation in each glass composition. Usually, these compounds can be found in 2 and 3 component phase diagrams. In case of glass containing more than 3 component (multicomponent), a normative calculation similar to the well known CIPW norm has to be performed.

2.3.1 Glass Containing 2 to 3 Component

The compounds in glass are basically the same as in a ceramic body. However, they are in a non-crystalline form. This leads to a reduced Gibbs free energy of formation. Usually, 2 to 3 component compound can be known from phase diagrams. Some phase diagrams are presented, i.e., the system of Na_2O-CaO-SiO_2, K_2O-Al_2O_3-SiO_2, CaO-

Al_2O_3-SiO_2. (see in the appendix)

2.3.2 Glass Containing More Than 3 Components

In case of glass types containing more than 3 components, the 3 component phase diagrams are insufficient although they still serve as a guide line. So, we do not know what kinds of compound will occur. However, they can be described by a predictive model called " CIPW norm" named after the petrologists Cross, Iddings, Pirsson, and Washinghton (Philpotts,1990). For glasses, we may use the same principle and develop a similar norm calculation. The sequence of compounds k is given on the following page, along with their molar masses M_k in g/mol and Gibbs free energy G_k in kJ/mol.

2.3.2.1 CIPW Norm Calculation.

To begin the CIPW norm calculation, the weight percentages of the oxides in the glass analysis are converted to molar proportions by dividing each oxide weight percent by its molecular weight. Using the formular in table 2.3, the molar proportions are distributed among the normative minerals according to the rules given below. The calculation can be carried out conveniently on a balance sheet, as shown in table 2.4. This norm is calculated by following step by step as

1. P_2O_5 is allotted to apatite (P_2O_5.3CaO), and CaO is reduced by 3 x P_2O_5.

2. Cr_2O_3 is allotted to Cr_2O_3.

3. The amount of (stoichiometric) Fe_2O_3 is split up in the two shares of Fe^{2+} (ferrous) and Fe^{3+}(ferric). The minimum of the two shares is allotted to FeO.Fe_2O_3. Residual ferric iron is allotted to Fe_2O_3, residual ferrous iron to FeO.SiO_2.

Table 2.3 Molar mass M_k in g/mol and Gibbs free energy G_k in kJ/mol of sequence compounds k.

compound k	M_k	$-G_k$ (dev)	$-G_k$ (s)	$-G_k$ (glassy)
$P_2O_5 \cdot 3CaO$	310.18	23.5	3895.7	3872.2
Cr_2O_3	151.99	20.7	1059.9	1039.2
Fe_2O_3	159.69	20.7	740.0	719.3
$FeO \cdot Fe_2O_3$	231.54	25.6	1014.4	988.7
$FeO \cdot SiO_2$	131.93	13.6	1119.0	1105.4
$MnO \cdot SiO_2$	131.02	13.6	1241.4	1227.8
$MgO \cdot SiO_2$	100.40	13.6	1462.9	1449.3
$2ZnO \cdot SiO_2$	222.82	18.5	1523.6	1505.1
$ZrO2 \cdot SiO_2$	183.30	29.3	3825.6	3796.2
$PbO \cdot SiO_2$	283.27	6.7	1067.1	1060.3
$CaO \cdot TiO_2$	135.98	25.6	1576.0	1550.4
BAS_2	375.47	42.9	4064.3	4021.4
$BaO \cdot 2SiO_2$	213.42	22.3	2415.7	2393.4
LAS_4	251.01	180.4	5758.3	5577.8
$Li2O \cdot SiO_2$	88.96	77.3	1543.4	1466.1
KAS_6	556.67	77.0	7482.1	7405.0
$K2O \cdot 2SiO_2$	154.29	5.5	2336.8	2331.3
NAS_6	524.44	92.1	7420.9	7328.8
CAS_2	278.21	45.0	4001.8	3956.8
$Al_2O_3 \cdot SiO_2$	162.05	29.3	2443.6	2414.2
$Na_2O \cdot 2B_2O_3$	201.22	16.2	3081.5	3065.3
B_2O_3	69.62	9.8	1192.8	1183.0
NC_3S_6	590.72	71.2	7913.3	7842.2
$Na_2O \cdot 2SiO_2$	182.15	36.8	2341.4	2304.7
SiO_2	60.08	8.0	857.1	849.0
NAS_2 *)	284.11	57.4	3990.1	3932.7
$Na_2O \cdot SiO_2$ *)	122.06	41.5	1470.4	1428.9
$CaO \cdot SiO_2$ *)	116.16	9.1	1551.1	1542.0
$2CaO \cdot SiO_2$ *)	172.24	14.0	2198.4	2184.4

*) These phases are to replace NAS_6, NS_2, and NC_3S_6 in the case of a silica deficiency and/or calcia excess;
dev: devitrification; s: most stable solid; glassy: a representative glassy state

G_k(dev) = Gibbs free energy of devitrification

G_k(s) = Gibbs free energy of crystal phase

G_k(glassy) = Gibbs free energy of glassy phase

Total silica is reduced accordingly.

4. TiO_2 is combined with CaO to form $CaO.TiO_2$ and CaO is reduced accordingly.

5. ZrO_2 is allotted to zircon ($ZrO_2.SiO_2$), and SiO_2 is reduced by ZrO_2.

6. The oxides MnO, MgO, ZnO and PbO are allotted to $MnO.SiO_2$, $MgO.SiO_2$, $2ZnO.SiO_2$ and $PbO.SiO_2$ respectively, and silica is reduced accordingly.

7. Li_2O is allotted to LAS_4, and Al_2O_3 is reduced by Li_2O, and silica is reduced by $4xLi_2O$. When $Al_2O_3 < Li_2O$, the remainder Li_2O is allotted to $Li_2O.SiO_2$.

8. K_2O is allotted to provisional orthoclase (KAS_6) and Al_2O_3 is reduced by K_2O, and SiO_2 is reduced by $6xK_2O$. The excess K_2O is allotted to $K_2O.SiO_2$ if Al_2O_3 is consumed.

9. BaO is allotted to BAS_2, and Al_2O_3 is reduced by BaO, and silica is reduced by 2xBaO. The excess BaO is allotted to $BaO.2SiO_2$ if Al_2O_3 is consumed.

10. If the Al_2O_3 remains form step 9, let it combine with an equal amount of Na_2O to form provisional albite (NAS_6), and silica is decreased by six times this amount. If there is insufficient Al_2O_3, proceed to step 12.

11. Al_2O_3 remaining from step 10 is combined with an equal amount of CaO to from provisinal anorthite (CAS_2), and silica is decreased by twice this amount. If Al_2O_3 exceeds CaO, it is calculated as mullite.

12. If Na_2O exceeds Al_2O_3 in step 10, an amount of B_2O_3 equal to the excess is allotted to $Na_2O.2B_2O_3$, and silica is decreased by two times this amount. The excess of B_2O_3 is allotted to B_2O_3.

13. If CaO from step 11 is still there, it is allotted to NC_3S_6.

14. If Na_2O still remains after step 13, the remaining Na_2O forms $Na_2O.2SiO_2$, and silica is reduced by the amount of the remaining Na_2O.

15. If SiO_2 is still positive, remaining SiO_2 is calculated as quartz.

16. If SiO_2 is negative, the rock contains insufficient silica for the provisionally formed silicate minerals. Some of these minerals must therefore be converted to ones containing less silica, until the silica deficiency is eliminated. The order in which this is done as follows: first, protoenstatite ($MgO.SiO_2$) is converted to olivine ($2MgO.SiO_2$), albite (NAS_6) to nepheline (NAS_2), orthoclase (KAS_6) to leucite (KAS_4), wollastonite to calcium orthosilicate ($2CaO.SiO_2$), leucite(KAS_4) to kaliophilite (KAS_2). Finally, anorthite CAS_2 to gehlenite C_2AS. For the glasses used here, the change KAS_6 ----> KAS_2 is done in one single step.

In an improved version, the three main oxides of the glass are determined first, the norm is performed according to the above rules, however, without allothing the reminders of the three main oxides. These are rather allotted strictly following the phase diagram.

Table 2.4 Balance sheet of CIPW norm calculation.

CIPW norm calculation

		SiO2	TiO2	ZrO2	Al2O3	B2O3	Fe2O3	FeO
g/100 g glass		51.00	0.40		6.70		2.40	
M(j) in g/mol		60.08	79.90	123.22	101.96	69.62	159.69	71.85
mol/100 g glass		0.84881	0.00501		0.06571		0.01503 Fe Ox	
P2O5·3CaO		¦	¦	¦	¦	¦	0.00902	0.01202
Cr2O3		¦	¦	¦	¦	¦	¦	¦
Fe2O3		¦	¦	¦	¦	¦	¦	¦
FeO·Fe2O3	0.00901	¦	¦	¦	¦	¦	*3*	-:-:-:-:¦
FeO·SiO2	0.00300	0.84581	<<<<<<	<<<<<<	<<<<<<	<<<<<<	<<<<<<	<<<<*4*
MnO·SiO2		0.84581	<<<<<<	<<<<<<	<<<<<<	<<<<<<	<<<<<<	<<<<<<
MgO·SiO2	0.32745	0.51835	<<<<<<	<<<<<<	<<<<<<	<<<<<<	<<<<<<	<<<<<<
2ZnO·SiO2		0.51835	<<<<<<	<<<<<<	<<<<<<	<<<<<<	<<<<<<	<<<<<<
ZrO2·SiO2		0.51835	<<<<<<	<<<<*8*	¦	¦		
PbO·SiO2		0.51835	<<<<<<	<<<<<<	<<<<<<	<<<<<<	<<<<<<	<<<<<<
CaO·TiO2	0.00500	¦	*10*	>>>>>>	>>>>>>	>>>>>>	>>>>>>	>>>>>>
CaF2		¦			¦	¦		
BAS2		0.51835	<<<<<<	<<<<<<	0.06571	-:-:-:-:	-:-:-:-:	-:-:-:-:
BaO·2SiO2		0.51835	<<<<<<	<<<<<<	<<<<<<	<<<<<<	<<<<<<	<<<<<<
LAS4		0.51835	<<<<<<	<<<<<<	0.06571	-:-:-:-:	-:-:-:-:	-:-:-:-:
Li2O·SiO2		0.51835	<<<<<<	<<<<<<	<<<<<<	<<<<<<	<<<<<<	<<<<<<
KAS6	0.01379	0.43555	<<<<<<	<<<<<<	0.05191	-:-:-:-:	-:-:-:-:	-:-:-:-:
K2O·2SiO2		0.43555	<<<<<<	<<<<<<	<<<<<<	<<<<<<	<<<<<<	<<<<<<
NAS6	0.00806	0.38715	<<<<<<	<<<<<<	0.04384	-:-:-:-:	-:-:-:-:	-:-:-:-:
CAS2	0.04384	0.29946	<<<<<<	<<<<<<		-:-:-:-:	-:-:-:-:	-:-:-:-:
Al2O3·SiO2		0.29946	<<<<<<	<<<<<<	<<<<*16*	¦		
Na2O·2B2O3		Rest!					-:-:-:-:	-:-:-:-:
B2O3						*17*		

2.4 Procedure of Theoretical Calculation

2.4.1 Creation of Stability Diagram.

From previous work on chemical durability of glasses (Paul, 1982), the stability diagram of some oxides were presented such as SiO_2, ZrO_2, Al_2O_3, PbO and ZnO. In this research work, 22 types of generally used oxides were used to create stability diagrams. These oxides can be classify into 5 groups. The first groups were R_2O_3 types: Al_2O_3, B_2O_3, Cr_2O_3 and Fe_2O_3. The second groups were RO_2 types:

SiO_2, TiO_2 and ZrO_2. The third groups were RO types: BaO, CaO, CdO, MgO, MnO, PbO, SrO, FeO and ZnO. The fourth groups were R_2O types: K_2O, Li_2O and Na_2O. The last groups were presented to allow for ions present in the aqueous solution such as CO_2 and P_2O_5 which can give CO_3^{2-} and PO_4^{3-} ions and their protonation steps.

After stability diagrams were created, the summary of hydration reactions of all oxides were presented at varied pH values; for a given oxide and pH range, only the species with maximum activity is given.

2.4.2 Predictive Model

A predictive model was set up in 4 steps :

(a) By following CIPW norm calculation rule, some parts were corrected to fit with glass (see 2.3.2.1), "CIPW calculation" program was created by using Lotus 123. The present thesis work partially contributed to set up this program. It is now avialable at the Department of Material Science. From this program, the constituting compounds in several type of glasses can be calculated.

(b) Calculate the Gibbs free energy G of hydration for selected oxide compounds at vary pH values; pH values are the upper limited of validity.

(c) 8 glass compositions (see 3.1.1) were used to calculate the compounds constituing the glasses.

(d) Create a predictive model for the calculation of the Gibbs free energy of formation of glass in term of kJ/100g of glass by using Lotus 123.

Table 2.5 Balance sheet for calculate dissolution Gibbs free energy

compound	mol/100g	checksum 99.905	component	wt. %	g/100g	mol/100g	dG(hydr)	n*dG(meta)
P2O5·3CaO			SiO2	51.00	51.00	0.85	-48.60	
Cr2O3			TiO2	0.40	0.40	0.01	14.49	
Fe2O3			ZrO2				89.12	
FeO·Fe2O3	0.0090		Al2O3	6.70	6.70	0.07	28.98	0.26
FeO·SiO2	0.0030		B2O3				-58.65	-0.18
MnO·SiO2			Fe2O3	2.40	2.40	0.02	-74.06	
MgO·SiO2	0.3275		Cr2O3				-69.41	-22.73
2ZnO·SiO2			P2O5				73.92	
ZrO2·SiO2			MgO	13.20	13.20	0.33	11.69	
PbO·SiO2			CaO	24.50	24.50	0.44	-0.61	
CaO·TiO2	0.0050		BaO				-61.62	-0.31
CaF2			MnO				49.23	
BAS2			ZnO				56.07	
BaO·2SiO2			PbO				-60.60	
LAS4			Li2O				-93.13	
Li2O·SiO2			Na2O	0.50	0.50	0.01	-191.22	
KAS6	0.0138		K2O	1.30	1.30	0.01	84.07	1.16
K2O·2SiO2			F2				-140.55	
NAS6	0.0081						48.83	0.39
CAS2	0.0438		total g	100.0	100.00	per mol	27.04	1.19
Al2O3·SiO2						58.11	68.47	
Na2O·2B2O3							-149.27	
B2O3							-43.36	
(metastable compounds)								
NC3S6							-175.26	
Na2O·2SiO2							-89.44	
SiO2	0.1054						14.58	1.54
CaO·SiO2							-41.99	
Na2O·SiO2							-167.74	
2CaO·SiO2	0.1940						-149.15	-28.94
(stable compounds)								
out of range	*						**********	
out of range	*						**********	
out of range	*						**********	
								-47.61

2.5 Results From Theory

2.5.1 Stability Diagram of Oxides Elements

Twenty two oxides were used to create stability diagrams which can be separated into 5 groups (see 2.4.1). The results of each groups are shown in the figures below:

The first groups : R_2O_3 types.

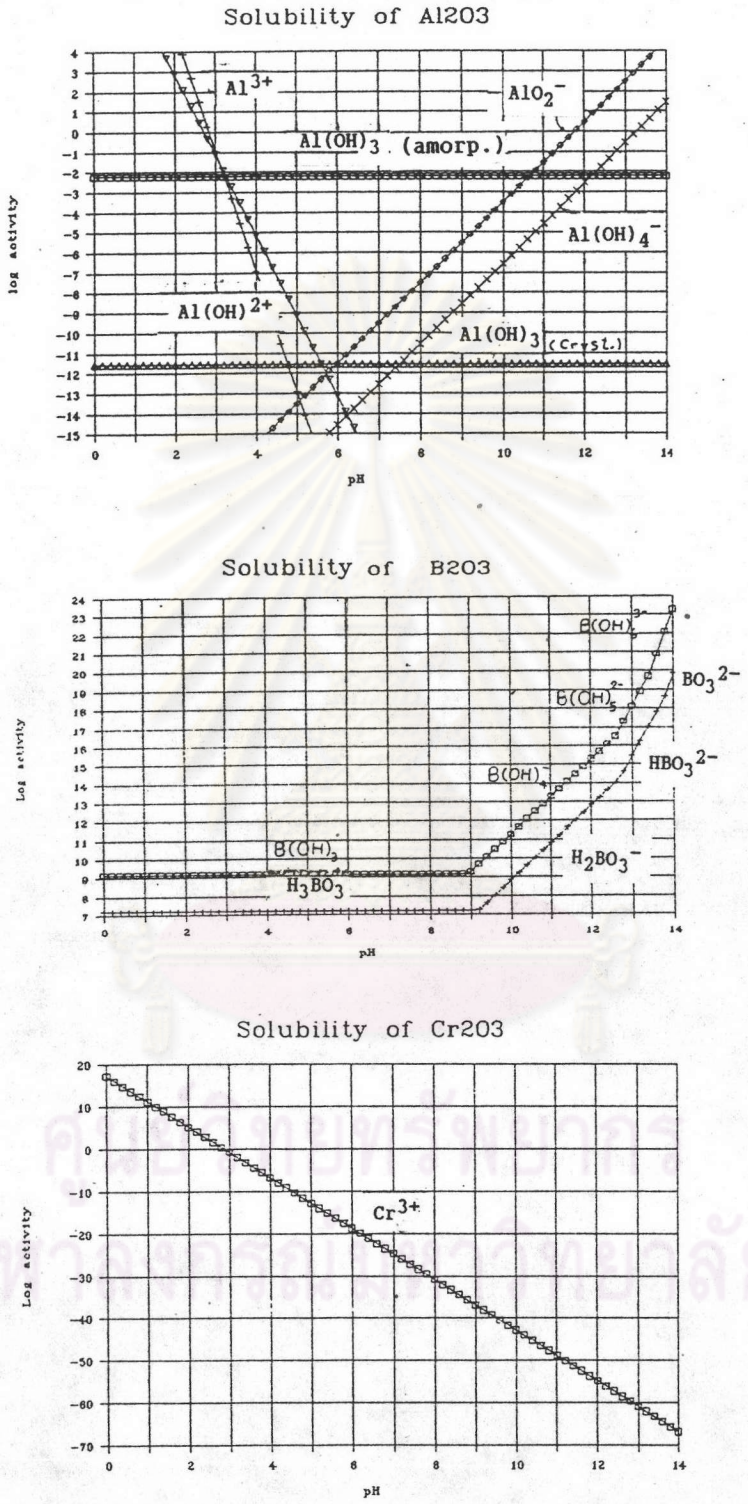

Fig. 2.8 Solubility diagram of Al_2O_3, B_2O_3, and Cr_2O_3 in vareous pH.

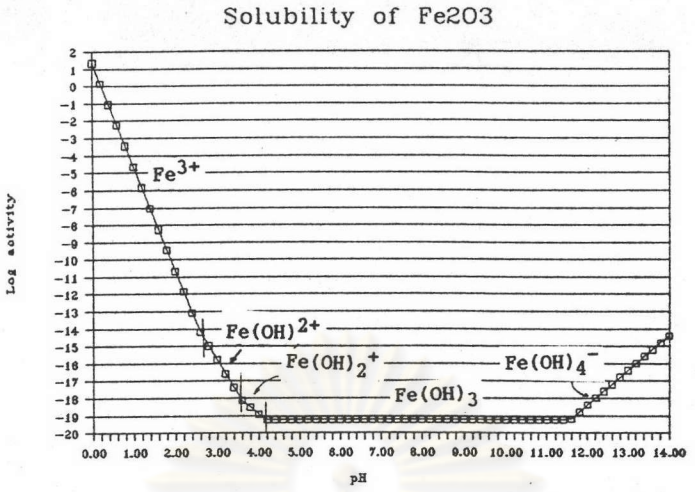

The second groups : RO_2 types.

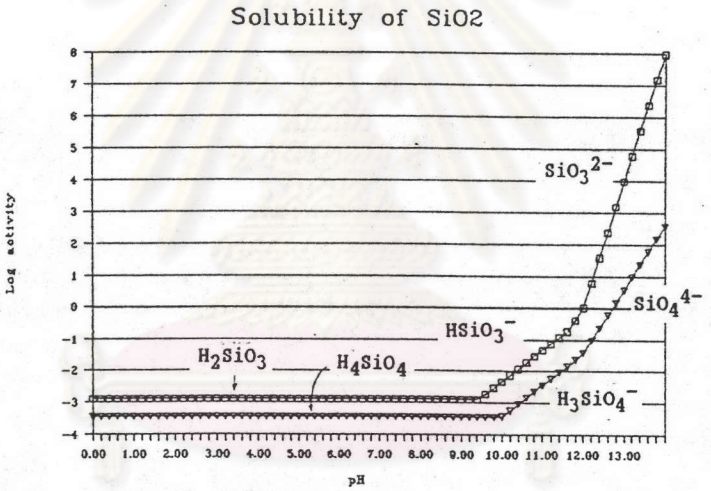

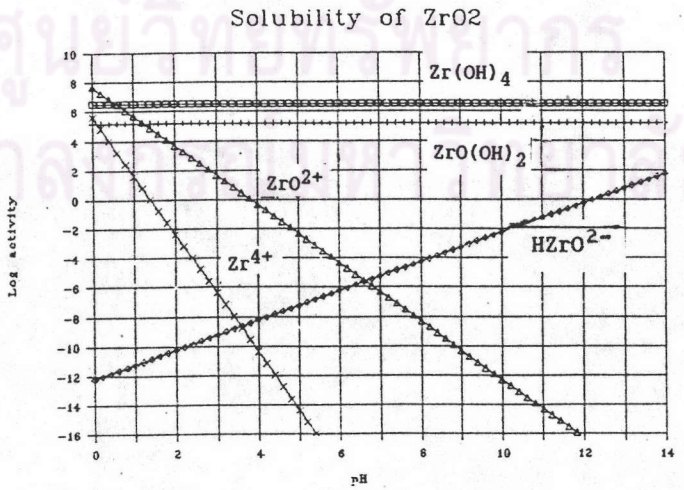

Fig. 2.9 Solubility diagram of Fe_2O_3, SiO_2 and ZrO_2 in various pH.

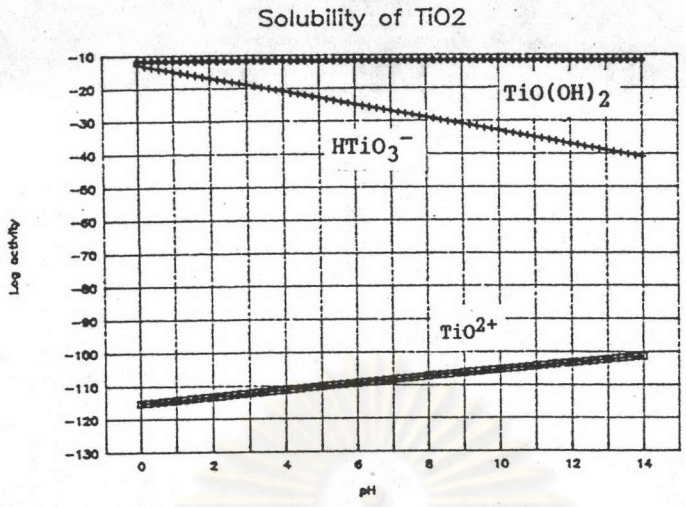

The Third groups : RO types.

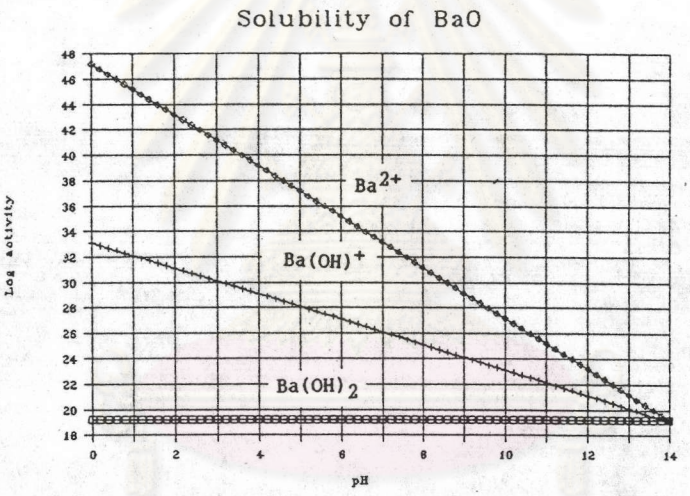

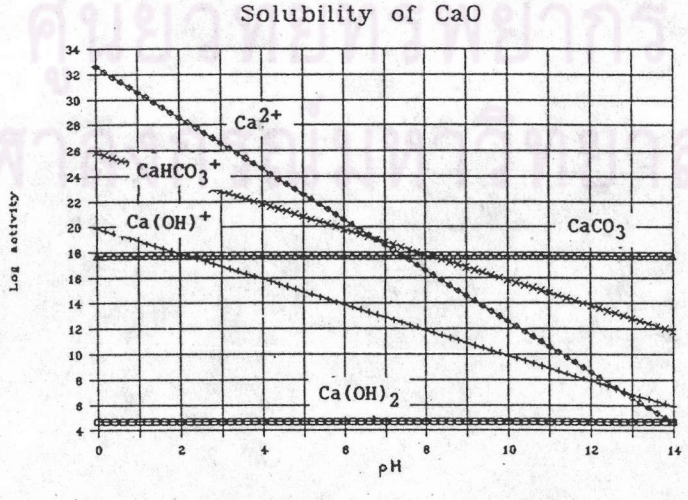

Fig. 2.10 Solubility diagram of TiO_2, BaO and CaO in various pH.

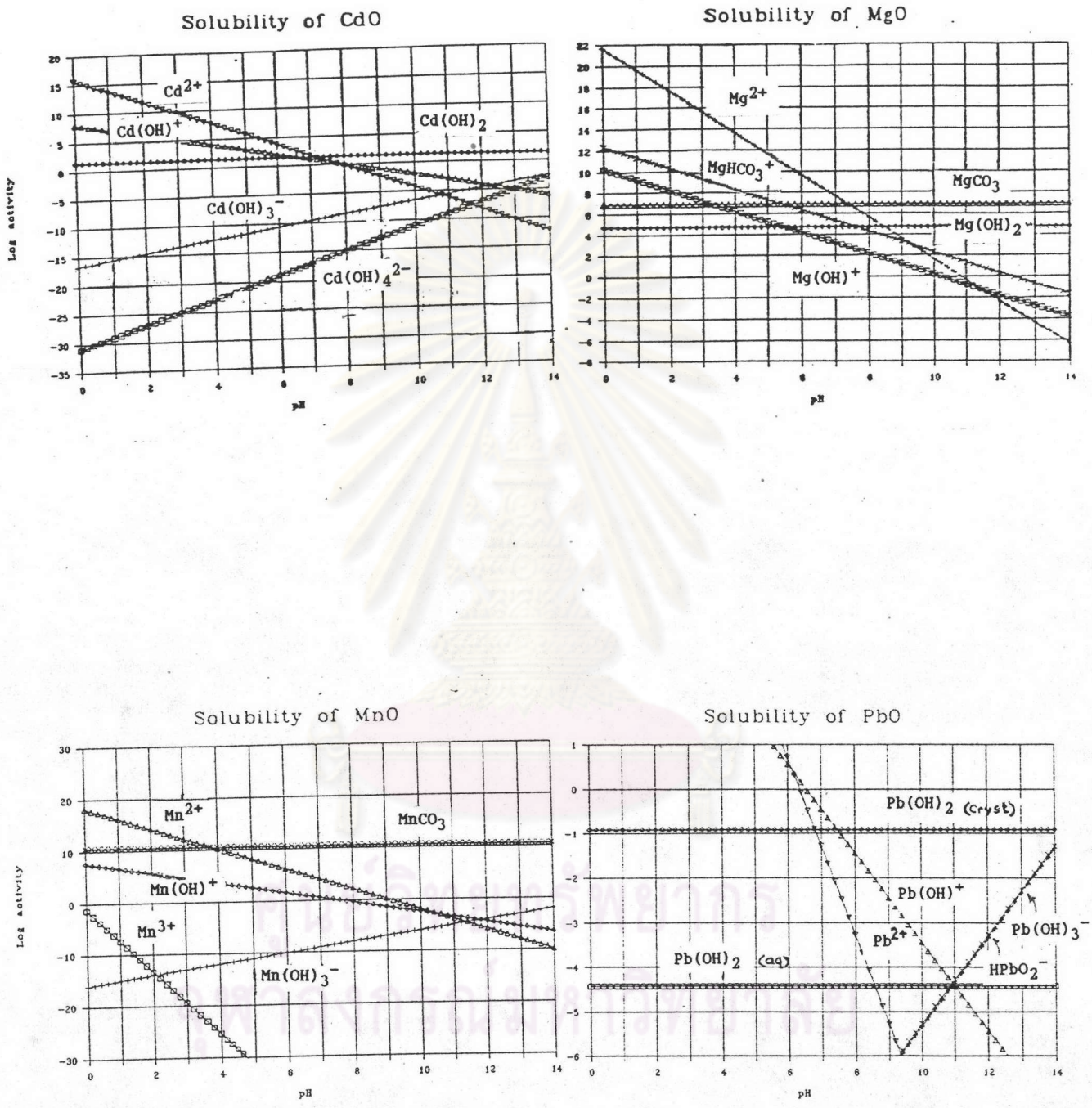

Fig. 2.11 Solubility diagram of CdO, MgO, MnO and PbO in various pH.

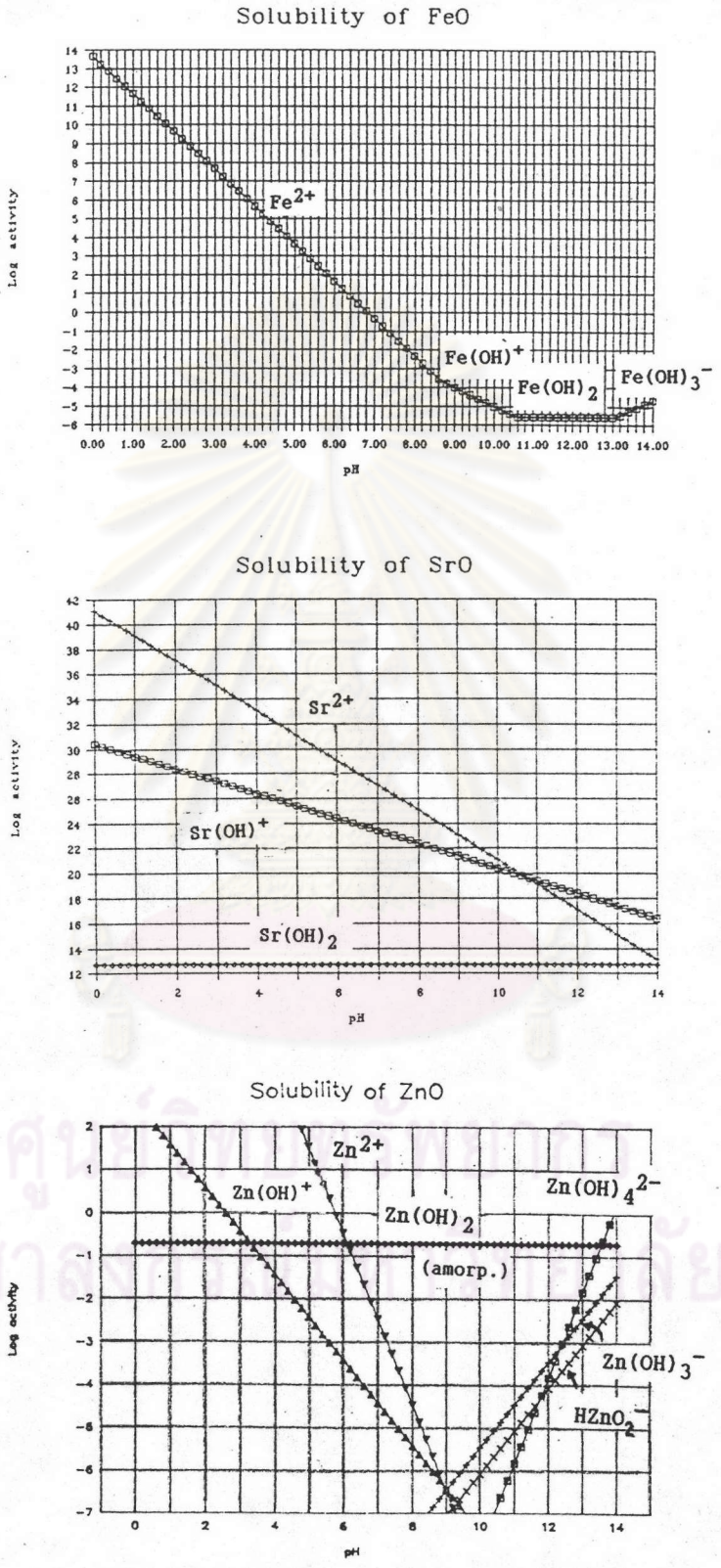

Fig. 2.12 Solubility diagram of FeO, SrO and ZnO in various pH.

The fourth groups : R_2O types.

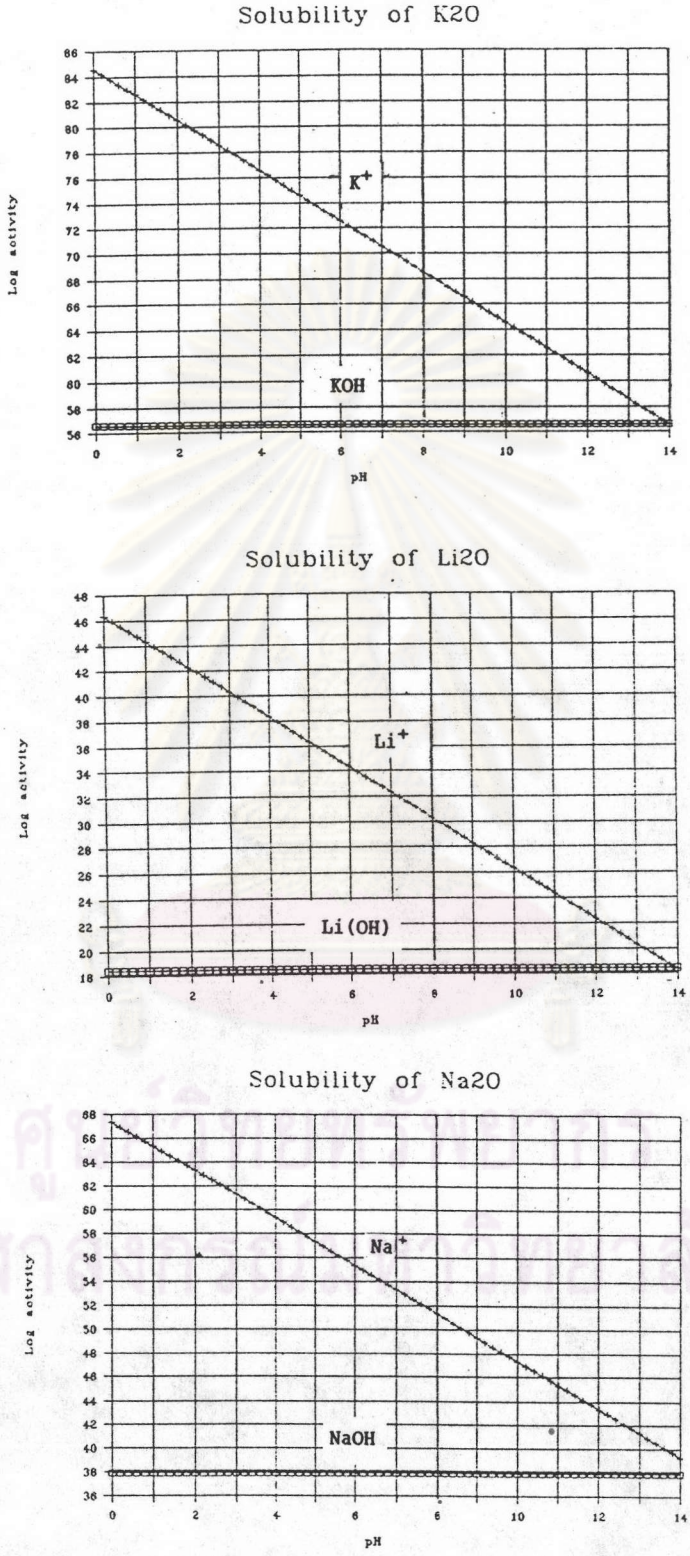

Fig. 2.13 Solubility diagram of K_2O,Li_2O and Na_2O in various pH.

The fifth groups

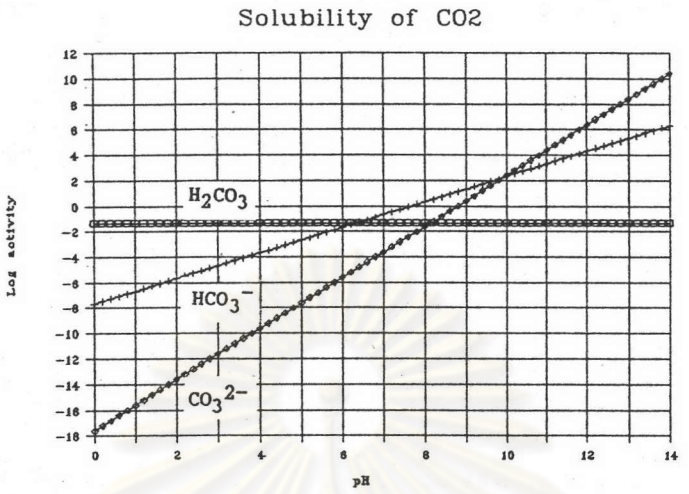

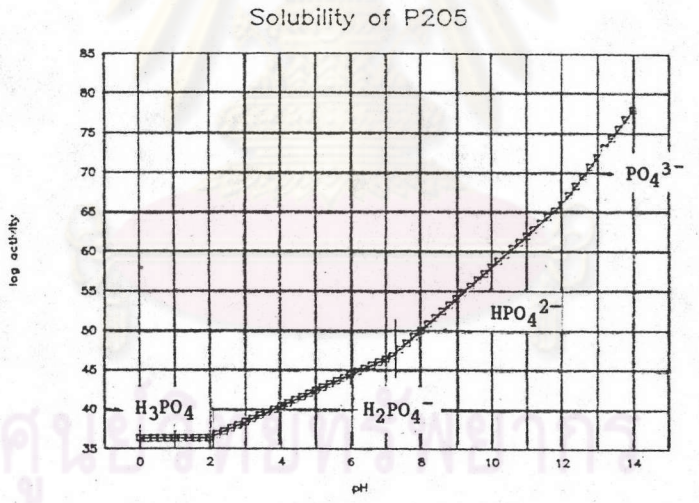

Fig. 2.15 Solubility diagram of CO_2 and P_2O_5 in various pH.

From the stability diagram, the summary of hydration reaction of all oxides are presented in the following table.

Table 2.6a Summary of hydration reactions of selected oxides for a given oxide and pH range.

SiO_2	$+ H_2O \longrightarrow H_2SiO_3$	$0.0 < pH < 9.6$
	$+ H_2O \longrightarrow H_2SiO_3^- + H^+$	$9.6 < pH < 11.8$
	$+ H_2O \longrightarrow SiO_3^{2-} + 2H^+$	$11.8 < pH < 14.0$
TiO_2	$+ H_2O \longrightarrow TiO(OH)_2$	
ZrO_2	$+ 2H^+ \longrightarrow ZrO^{2+} + H_2O$	$0.0 < pH < 0.5$
	$+ 2H_2O \longrightarrow Zr(OH)_4$	$0.5 < pH < 14.0$
Al_2O_3	$+ 6H^+ \longrightarrow 2Al^{3+} + 3H_2O$	$0.0 < pH < 3.2$
	$+ 3H_2O \longrightarrow 2Al(OH)_3$	$3.2 < pH < 10.6$
	$+ H_2O \longrightarrow 2AlO^-_2 + 2H^+$	$10.6 < pH < 14.0$
B_2O_3	$+ 3H_2O \longrightarrow 2H_3BO_3$	$0.0 < pH < 9.2$
	$+ 3H_2O \longrightarrow 2H_2BO_3^- + 2H^+$	$9.2 < pH < 12.6$
	$+ 3H_2O \longrightarrow 2HBO_3^{2-} + 4H^+$	$12.6 < pH < 13.8$
	$+ 3H_2O \longrightarrow 2BO_3^{3-} + 6H^+$	$13.8 < pH < 14.0$
Fe_2O_3	$+ 6H^+ \longrightarrow 2Fe^{3+} + 3H_2O$	$0.0 < pH < 2.6$
	$+ H_2O + 2H^+ \longrightarrow 2Fe(OH)_2^+$	$2.6 < pH < 4.1$
	$+ 3H_2O \longrightarrow 2Fe(OH)_3$	$4.1 < pH < 11.6$
	$+ 5H_2O \longrightarrow 2Fe(OH)_4^- + 2H^+$	$11.6 < pH < 14.6$
Cr_2O_3	$+ 6H^+ \longrightarrow 2Cr^{2+} + 3H_2O$	
P_2O_5	$+ 3H_2O \longrightarrow 2H_3PO_4$	$0.0 < pH < 2.0$
	$+ 3H_2O \longrightarrow 2H_2PO_4^- + 2H^+$	$2.0 < pH < 7.2$
	$+ 3H_2O \longrightarrow 2HPO_4^{2-} + 4H^+$	$7.2 < pH < 12.0$
	$+ 3H_2O \longrightarrow 2PO_4^{3-} + 6H^+$	$12.0 < pH < 14.0$

Table 2.6b Summary of hydration reactions of selected oxides for a given oxide and pH range.

MgO	$+ 2H^+ \longrightarrow Mg^{2+} + H_2O$	$0.0 < pH < 7.5$
	$+ H_2O \longrightarrow Mg(OH)_2$	$7.5 < pH < 14.0$
	$+ HCO_3^- + 2H^+ \longrightarrow MgHCO_3^+ + H_2O$	$0.0 < pH < 5.5$
	$+ HCO_3^- + H^+ \longrightarrow MgCO_3 + H_2O$	$5.5 < pH < 14.0$
CaO	$+ 2H^+ \longrightarrow Ca^{2+} + H_2O$	$0.0 < pH < 12.9$
	$+ H^+ \longrightarrow CaOH^+$	$12.9 < pH < 14.0$
	$+ 2H^+ \longrightarrow Ca^{2+} + H_2O$	$0.0 < pH < 6.5$
	$+ HCO_3^- + 2H+ \longrightarrow CaHCO_3^+ + H_2O$	$6.5 < pH < 8.1$
	$+ HCO_3^- + H^+ \longrightarrow CaCO_3 + H_2O$	$8.1 < pH < 14.0$
BaO	$+ 2H^+ \longrightarrow Ba^{2+} + H_2O$	
MnO	$+ 2H^+ \longrightarrow Mn^{2+} + H_2O$	$0.0 < pH < 10.6$
	$+ H^+ \longrightarrow Mn(OH)^+$	$10.6 < pH < 11.8$
	$+ 2H_2O \longrightarrow Mn(OH)_3^- + H^+$	$11.8 < pH < 14.0$
	$+ 2H^+ \longrightarrow Mn^{2+} + H_2O$	$0.0 < pH < 3.9$
	$+ HCO_3^- + H^+ \longrightarrow MnCO_3 + H_2O$	$3.9 < pH < 14.0$
FeO	$+ 2H^+ \longrightarrow Fe^{2+} + H_2O$	$0.0 < pH < 8.8$
	$+ H^+ \longrightarrow Fe(OH)^+$	$8.8 < pH < 10.6$
	$+ H_2O \longrightarrow Fe(OH)_2$	$10.6 < pH < 13.0$
	$+ 2H_2O \longrightarrow Fe(OH)_3^- + H^+$	$13.0 < pH < 14.0$
	$+ 2H^+ \longrightarrow Fe^{2+} + H_2O$	$0.0 < pH < 3.8$
	$+ HCO_3^- + H^+ \longrightarrow FeCO_3 + H_2O$	$3.8 < pH < 14.0$

Table 2.6c Summary of hydration reactions of selected oxides for a given oxide and pH range.

ZnO	$+ 2H^+ \longrightarrow Zn^{2+} + H_2O$	$0.0 < pH < 5.5$
	$+ H_2O \longrightarrow Zn(OH)_2$	$5.5 < pH < 14.0$
	$+ 2H^+ \longrightarrow Zn^{2+} + H_2O$	$0.0 < pH < 3.8$
	$+ HCO_3^- + H^+ \longrightarrow ZnCO_3 + H_2O$	$3.8 < pH < 14.0$
PbO	$+ 2H^+ \longrightarrow Pb^{2+} + H_2O$	$0.0 < pH < 6.3$
	$+ H^+ \longrightarrow Pb(OH)^+$	$6.3 < pH < 7.6$
	$+ H_2O \longrightarrow Pb(OH)_2$	$7.6 < pH < 14.0$
	$+ 2H+ \longrightarrow Pb^{2+} + H_2O$	$0.0 < pH < 2.9$
	$+ HCO_3^- + H^+ \longrightarrow PbCO_3 + H_2O$	$2.9 < pH < 14.0$
CdO	$+ 2H^+ \longrightarrow Cd^{2+} + H_2O$	$0.0 < pH < 7.4$
	$+ H_2O \longrightarrow Cd(OH)_2$	$7.4 < pH < 14.0$
	$+ 2H^+ \longrightarrow Cd^{2+} + H_2O$	$0.0 < pH < 3.8$
	$+ HCO_3^- + H^+ \longrightarrow CdCO_3 + H_2O$	$3.8 < pH < 14.0$
Li_2O	$+ 2H^+ \longrightarrow 2Li^+ + H_2O$	
Na_2O	$+ 2H^+ \longrightarrow 2Na^+ + H_2O$	
K_2O	$+ 2H^+ \longrightarrow 2K^+ + H_2O$	
CO_2	$+ H_2O \longrightarrow H_2CO_3$	$0.0 < pH < 6.5$
	$+ H_2O \longrightarrow HCO_3^- + H^+$	$6.5 < pH < 9.8$
	$+ H_2O \longrightarrow CO_3^{2-} + 2H^+$	$9.8 < pH < 14.0$

2.5.2 Results for the Hydration Reaction of Individual Oxides

Gibbs free energies of hydration change considerably with pH (see table 2.7) they do not change gradually, but rather abruptly when a stability limit for a certain species is exceeded. The sudden precipitation of a solid phase or color change of an indicator is familiar examples for such abrupt changes of speciation. For the experiments in Gamble's solution, the pH range of approx. 6 to 9.5 shall be considered as relevant; 6 stands for the pH of natural water, and 9.5 for a slight accumulation of leached alkali. Within this range, most glass compounds exhibit one species only. This is not the case for compounds containing MgO, CaO, or P_2O_5. Since MgO and CaO are major glass components, their behavior needs to be discussed in detail. Figures 2.10 and 2.11 show the so-called solubility diagrams for CaO and MgO respectively, in the pH range 0 to 14. Both oxides display changes of the predominant Ca^{2+} and Mg^{2+} species in the pH range of 0-12.5 and 0-8.5 respectively. If CO_2 saturation occurs, a species of $CaHCO_3^+$, $CaCO_3$ and $MgCO_3$ will predominate in the range of pH 6.5-8.2, 8.2-14 and 7.5-14, respectively. This makes compound more stable than in the absence of no CO_2 saturation. The formation of $CaCO_3$ or $MgCO_3$, however, requries enough Mg^{2+}, Ca^{2+} and CO_3^{2-}, so that the respective solubility limits are exceeded.

2.5.3 Glass Constituting Compounds and dissolution Gibbs free energy of glasses.

After a CIPW norm was developed and a predictive model was created, 8 glass compositions were used to calculate the influence of compounds and the Gibbs free energy of formation of glasses as shown in the following table.

Table 2.7a Gibbs free energy of hydration for selected oxide compounds at varied pH.

compound	pH	G in kJ/mol
$P_2O_5 \cdot 3CaO$	1.5	-73.13
	7.2	-48.60
	12.0	33.70
	12.6	174.68
	14.0	153.83
Cr_2O_3	3.0	-119.31
	14.0	14.49
	log K	-2.54
Fe_2O_3	2.6	-28.34
	4.1	41.68
	11.6	89.12
	14.0	61.49
$FeO \cdot Fe_2O_3$	2.6	-88.48
	4.1	-18.46
	8.8	28.98
	10.6	78.49
	11.6	138.55
	13.0	110.92
	14.0	106.10
$FeO \cdot SiO_2$	8.8	-58.65
	9.6	-9.15
	10.6	46.65
	11.8	26.81
	13.0	13.46
	14.0	8.64
$MnO \cdot SiO_2$	9.6	-74.06
	11.8	42.22
	14.0	3.75
$MgO \cdot SiO_2$	8.2	-69.41
	9.6	18.01
	11.6	-6.09
	14.0	-19.44
$2ZnO \cdot SiO_2$	5.5	-98.49
	9.6	73.92
	11.8	49.82
	14.0	36.47

compound	pH	G in kJ/mol
$ZrO2 \cdot SiO_2$	0.5	9.34
	9.6	11.69
	11.8	-12.41
	14.0	-25.76
$CaO \cdot TiO_2$	12.6	-61.62
	14.0	11.33
CaF_2	4.0	12.98
	14.0	
BAS_2	3.2	-128.96
	9.6	56.07
	10.6	167.67
	11.8	93.50
	14.0	66.76
$BaO \cdot 2SiO_2$	9.6	-60.60
	11.8	51.00
	14.0	24.26
KAS_6	3.2	-100.96
	9.6	84.07
	10.6	99.27
	11.8	25.14
	14.0	-54.96
$K_2O \cdot 2SiO_2$	9.6	-140.55
	11.8	-28.95
	14.0	-55.65
NAS_6	3.2	-136.20
	9.6	48.83
	10.6	64.03
	11.8	-20.00
	14.0	-90.20
NAS_2	3.2	-194.56
	9.6	-9.53
	10.6	102.07
	11.8	27.94
	14.0	1.24

Table 2.7b Gibbs free energy of hydration for selected oxide compounds at varied pH.

compound	pH	G in kJ/mol
CAS_2	3.2	-198.68
	7.0	-13.65
	9.6	27.04
	10.6	138.64
	11.8	-15.39
	14.0	-42.09
$Al_2O_3 \cdot SiO_2$	3.2	-116.56
	9.6	68.47
	10.6	44.37
	11.8	-29.76
	14.0	-43.11
$Na_2O \cdot 2B_2O_3$	9.2	-149.27
	12.6	-104.68
	13.8	-136.67
	14.0	-150.07
B_2O_3	9.2	-43.36
	12.6	-100.97
	13.8	-116.96
	14.0	-123.66
NC_3S_6	7.0	-297.32
	9.6	-175.26
	11.8	79.64
	14.0	-0.46
$Na_2O \cdot 2SiO_2$	9.6	-89.44
	11.8	22.16
	14.0	-4.51
$Na_2O \cdot SiO_2$	9.6	-167.74
	11.8	-111.73
	14.0	-45.17
$CaO \cdot SiO_2$	7.0	-82.68
	9.6	-41.99
	11.8	13.81
	14.0	0.46
$2CaO \cdot SiO_2$	7.0	-230.53
	9.6	-149.15
	11.8	-93.25
	14.0	-26.79
SiO_2	9.6	14.58
	11.8	-9.51
	14.0	-22.85
$M_3S_2H_2$ chrysotile[a]	8.2	-159.29
	9.6	102.96
	11.8	54.76
	14.0	-28.06
$M_{48}S_{34} \cdot H_{31}$ antigorite[b]	8.2	-2431.85
	9.6	1764.21
	11.8	944.81
	14.0	490.91
$M_4S_6H_7$ sepiolite[c]	8.2	-153.25
	9.6	196.43
	11.8	51.83
	14.0	-28.27

a) $Mg_3Si_2O_5(OH)_4$
b) $Mg_{48}Si_{34}O_{85}(OH)_{62}$
c) $Mg_4Si_6O_{15}(OH)_2(OH_2)_2(OH_2)_4$

Table 2.8 Compounds constituing the glasses.

Compounds	JM1	JM2	B1	B2	S1	S2	E1	E2
FeO.Fe2O3	0.05	0.05	10.79	10.89	0.02	0.02	0.02	0.02
FeO.SiO2	0.01	0.01	2.05	2.07	-.-	-.-	-.-	-.-
MgO.SiO2	7.77	0.12	10.51	23.19	11.38	0.10	11.81	0.15
CaO.TiO2	0.10	0.10	4.99	4.95	1.21	1.21	0.07	0.07
KAS6	5.97	5.91	8.21	8.33	-.-	-.-	-.-	-.-
NAS6	20.81	20.77	24.45	24.63	-.-	-.-	3.38	3.38
Na2O.2B2O3	6.99	6.95	-.-	-.-	-.-	-.-	-.-	-.-
B2O3	-.-	-.-	-.-	-.-	-.-	-.-	8.07	8.06
Na2O.2SiO2	25.91	22.62	-.-	-.-	-.-	-.-	-.-	-.-
NC3S6	21.80	32.68	-.-	-.-	-.-	-.-	-.-	-.-
CAS2	-.-	-.-	13.15	10.52	14.29	18.56	37.01	36.98
C2AS	-.-	-.-	6.73	9.52	29.60	25.39	-.-	-.-
CaO.SiO2	-.-	-.-	18.62	5.39	43.49	54.72	20.85	30.66
SiO2	10.58	10.78	-.-	-.-	-.-	-.-	18.79	20.68
Sum	99.99	99.99	99.50	99.49	99.99	100.00	100.00	100.00

Table 2.9a Dissolution Gibbs free energy
a = N2 bubble(pH 8.5), 0.026 CO2
b = N2 bubble(pH 8.5), 0.026 CO2, RCO3 and Mg(OH)2
c = N2 bubble(pH 8.5), 0.026 CO2 and C-S-H phase formation
d = N2 bubble(pH 8.5), 0.026 CO2,RCO3,Mg(OH)2 and C-S-H phase formation
e = Binder (pH 9.5), 0.05 CO2, and Mg(OH)2
f = Binder (pH 9.5), 0.05 CO2, Mg(OH)2 and C-S-H phase

Types	V(N2)	a*	b	c	d	V(BD)	e	f*
JM1	23.0	-34.4	-23.5	-26.0	-22.1	22.9	-36.8	-27.5
JM2	16.9	-32.3	-21.7	-19.8	-19.7	16.4	-41.6	-27.6
B3	7.9	-22.8	0.7	-8.6	3.0	4.8	-4.4	11.5
B4	9.2	-21.0	5.3	1.0	6.2	7.3	-14.0	10.5
S1	9.6	-58.5	-11.9	-14.8	-4.8	5.7	-53.2	-4.6
S2	7.3	-56.5	-10.5	-12.9	-3.4	6.1	-61.5	-12.8
E1	6.7	-23.8	1.8	-0.3	5.6	4.5	-25.0	1.2
E2	5.5	-22.3	2.7	7.5	7.5	2.7	-34.1	-0.8

Table 2.9b Dissolution Gibbs free energy
a = Gamble's, 0.05 CO2
b = Gamble's, 0.05 CO2, RCO3 and Mg(OH)2
c = Gamble's, 0.05 CO2 and C-S-H phase formation
d = Gamble's, 0.05 CO2, RCO3, Mg(OH)2 and C-S-H phase formation
e = Buffer (pH5)
f = Buffer (pH5) and C-S-H phase formation
g = Buffer (pH5)---> take alkali out (leaching)

Types	V(Gam)	a*	b	c	d	V(pH5)	e*	f	g*
JM1	22.3	-33.3	-31.7	-25.1	-23.9	0.5	-33.2	-25.0	2.0
JM2	13.1	-30.9	-30.2	-18.6	-18.6	0.5	-30.8	-18.5	3.8
B3	4.9	-24.2	-20.0	-10.2	-6.8	5.9	-24.5	-10.5	-19.2
B4	7.3	-21.8	-19.0	-0.2	1.3	45.8	-22.1	-0.5	-17.1
S1	7.6	-58.2	-53.7	-15.2	-13.3	2940.0	-58.1	-15.3	-58.1
S2	4.7	-55.8	-52.6	-12.9	-12.2	2780.0	-55.7	-12.9	-55.7
E1	4.6	-22.5	-19.5	0.5	2.3	1.8	-22.5	0.5	-19.2
E2	3.4	-20.5	-18.9	8.6	8.7	1.3	-20.5	8.7	-17.1
JM-104	0.9	-8.7	-.-	-.-	-.-	-.-	-.-	-.-	-.-
E-104	0.2	-18.3	-.-	-.-	-.-	-.-	-.-	-.-	-.-
Diabase	1.1	-33.9	-.-	-.-	-.-	-.-	-.-	-.-	-.-
TEL	3.5	-31.5	-.-	-.-	-.-	-.-	-.-	-.-	-.-
Slag	0.7	-55.4	-.-	-.-	-.-	-.-	-.-	-.-	-.-
Basalt	1.1	-12.4	-.-	-.-	-.-	-.-	-.-	-.-	-.-
Erionite	0.0	13.1	-.-	-.-	-.-	-.-	-.-	-.-	-.-

2.6 Discussion of Results From Theory

2.6.1 General Form of Solubility Diagram.

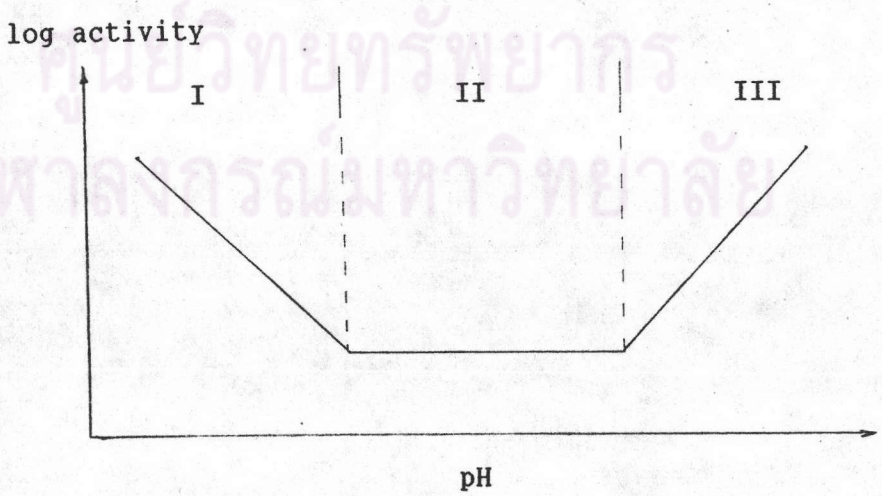

Fig 2.15 Solubility diagram plots of pH and log acivity.

Most of all stability diagrams can be described in three pH ranges. The first range is an acid unstable range. Species of R^{3+}, R^{2+} and R^{+} are predominant. The second range is a stable range with completely hydrated species $R(OH)_n$, H_nRO_n or H_mRO_n such as $Al(OH)_3$, H_3BO_3 or H_2SiO_3 respectively. The third range is a basic unstable range. Deprotonated species are predominant such as $Al(OH)_4^-$, HBO_3^{2-}, SiO_3^{2-}, or $Pb(OH)_3^-$. The slopes of the unstable ranges are dependent on the amounts of proton excess or deficiency; the location relative to the pH scale is a function of the specific oxide. For example, within the range $0<pH<14$, SiO_2 exhibits the stable and the basic unstable ranges only, while alkali oxides show nothing else but the acid unstable range.

Another way of presentation of a speciation diagram is created by plotting the relative amount in % of aqueous species versus pH as showed in the following figure.

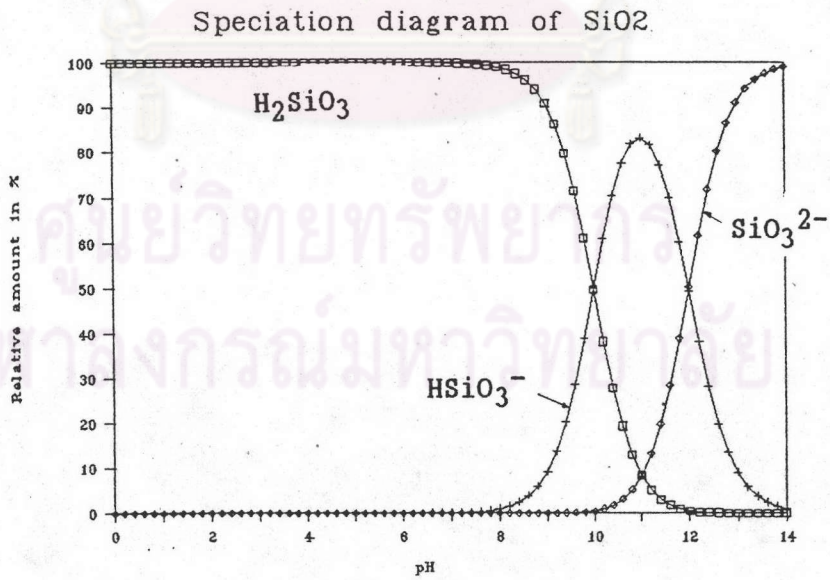

Fig. 2.16 Speciation diagram of SiO_2.

From the above figure, in the range of pH 0 - 7.4 100% H_2SiO_3 predominates. At pH 11, 10% of SiO_3^{2-} and H_2SiO_3 species and 80% of $HSiO_3^-$ species are present.

2.6.2 Gibbs Free Energy of Hydration and Preditive Criteria.

The set of compounds k which are used as a base to calculate the CIPW norm is listed in the table 2.3. The compounds listed above SiO_2 are usually sufficient for commercial glasses. The further compounds are needed to allow for extremely high (Na_2O + CaO) per SiO_2 ratio. In table 2.3 as well as throughout the report, the shorthand notation N = Na_2O, K = K_2O, M = MgO, C = CaO, B = BaO, A = Al_2O_3, S = SiO_2 is eventually used.

After the norm calculation as described in 2.3.2 is performed, the results are presented in terms of glass-constituting compounds k as listed in table 2.8. Different degrees of acidity appear as district changes in the pattern of compounds. In the sub-system N-A-C-S, to basic glasses show the compounds NAS_6, CAS_2, C_2AS and CS. For E glass boron was present in B_2O_3 instead of $Na_2O.2B_2O_3$ because Na_2O was used to form NAS_6. This is compatible with the general finding that alkali satisfies the demand of alumina first (bringing about the change from $[AlO_6]$ to $[AlO_4]R$) ; only the remainder of alkali R associates with B to bring about the change from $[BO_3]$ to $[BO_4]R$.

From table 2.9a and 2.9b, dissolution Gibbs free energy in kJ per 100 g of glasses was calculated at 4 different pH 7.6, 8.5, 5.0 and 9.5 for the condition of Gamble's solution, Gamble's saturated with N2, buffer solution and Gamble's solution with samples coated with binder respectively. These calculations used 0.05 bar of CO_2 (for pH 7.6 and 9.5) and 0.026 bar for pH 8.5 (calculated from the

amount of carbonate in the solution). Moreover, the effects of RCO_3, $Mg(OH)_2$ and C-S-H phase formation in case of binder or the fast dissolution of CaO rich glass were evaluated. The G values cover the range of 9 to -57 kJ/100g for glasses pH 7.6 and 8.5. Fibre samples (Scholze and Conradt, 1987) were also used to compare.